

This is the accepted manuscript made available via CHORUS. The article has been published as:

Invariance of Topological Indices Under Hilbert Space Truncation

Zhoushen Huang, W. Zhu, Daniel P. Arovas, Jian-Xin Zhu, and Alexander V. Balatsky
Phys. Rev. Lett. **120**, 016403 — Published 5 January 2018

DOI: [10.1103/PhysRevLett.120.016403](https://doi.org/10.1103/PhysRevLett.120.016403)

Invariance of topological indices under Hilbert space truncation

Zhoushen Huang,¹ W. Zhu,² Daniel P. Arovas,³ Jian-Xin Zhu,⁴ and Alexander V. Balatsky^{1,5}

¹*Institute for Materials Science, Los Alamos National Laboratory, Los Alamos, NM 87545, USA**

²*T-4 and CNLS, Los Alamos National Laboratory, Los Alamos, NM 87545, USA†*

³*Department of Physics, University of California San Diego, La Jolla, CA 92093, USA‡*

⁴*T-4 and CINT, Los Alamos National Laboratory, Los Alamos, NM 87545, USA§*

⁵*NORDITA, Roslagstullsbacken 23, SE-106 91 Stockholm, Sweden¶*

(Dated: December 11, 2017)

We show that the topological index of a wavefunction, computed in the space of twisted boundary phases, is preserved under Hilbert space truncation, provided the truncated state remains normalizable. If truncation affects the boundary condition of the resulting state, the invariant index may acquire a different physical interpretation. If the index is symmetry protected, the truncation should preserve the protecting symmetry. We discuss implications of this invariance using paradigmatic integer and fractional Chern insulators, Z_2 topological insulators, and Spin-1 AKLT and Heisenberg chains, as well as its relation with the notion of bulk entanglement. As a possible application, we propose a partial quantum tomography scheme from which the topological index of a generic multi-component wavefunction can be extracted by measuring only a small subset of wavefunction components, equivalent to the measurement of a bulk entanglement topological index.

Introduction—The investigation of topological phases and their classification [1–4] has grown into a major endeavor in condensed matter physics, thanks to rapid advancements in material realization [5, 6] and experimental platforms for “quantum simulation” such as ultra cold atomic systems [7–9]. The appeal of topology is that related physical quantities, for example quantized Hall conductance [10] and charge polarization [11, 12], can be formulated as discrete topological indices, which are thus robust against continuous deformations of the system.

A topological index is fundamentally a property of a wavefunction. Yet apart from free fermions and a few exactly solvable models, it is impractical to obtain an exact wavefunction through the diagonalization of a Hamiltonian. One alternative is to build candidate wavefunctions through projective construction, whereby a parent state defined in a larger Hilbert space is linked to a projected state in a smaller, truncated Hilbert space [13–15]. Both the parent and the truncated Hilbert spaces can play the role of the physical space. For example, a matrix product state is constructed by projecting a parent state, defined in a tensor product of site Hilbert spaces, onto bond Hilbert spaces, where truncation in bond dimension is implemented according to the entanglement content [16]. In this case, the parent space is physical, while the projected state offers a more economical description suitable for numerical solution. In parton-type constructions [17], on the other hand, one first fractionalizes the physical degrees of freedom into partons, with which a mean field state can be written down in the enlarged parton Hilbert space, then a Gutzwiller type projection is employed to pull the state back to the physical space. In this case, the truncated space is physical, while the enlarged space provides a more natural platform for exotic phenomena such as fractionalization. Treated as variational ansatz, the projected wavefunctions thus obtained can be further optimized for better approximation of target states, yet for the issue of topological characterization, a fundamental question remains rarely touched: how does the truncation procedure

itself affect topology?

In this work, we investigate the connection between Hilbert space truncation and topology on the wavefunction level. Specifically, we address the question: what is the relation between the parent and the projected wavefunctions in terms of their topological index? The topological indices we will consider are those that can be computed via the formalism of twisted boundary phases [18], such as integer and fractional Chern numbers, quantized Berry phase, and various symmetry protected Z_2 indices. We will assume that the parent state is a gapped eigenstate $|\Psi(\kappa)\rangle$ of a many-body Hamiltonian, hence it has well-defined topological indices. Here $\kappa \equiv (\kappa_1, \kappa_2, \dots)$ are the boundary phases implemented as $a_{\mathbf{r}+N_i\hat{e}_i}^+ = a_{\mathbf{r}}^+ e^{ik_i}$, where $a_{\mathbf{r}}^+$ is a fermionic/bosonic creation operator or a spin raising operator on lattice site \mathbf{r} , and N_i is the linear size along direction \hat{e}_i . The full parameter space of κ , with $\kappa_i \in [0, 2\pi)\forall i$, will be referred to as a “Brillouin Zone” (BZ). We will show that the topological index of $|\Psi\rangle$ is fully preserved by its truncated version, $|\tilde{\Psi}\rangle = P|\Psi\rangle / \sqrt{\langle\Psi|P|\Psi\rangle}$, if both indices are computed using the *same* κ BZ, provided the κ -independent projection P fulfills the following conditions: (1) At no point in the κ BZ does the truncated wavefunction become a null vector, whereby information of the parent state is fully lost. (2) For a parent state belonging to symmetry protected topological classes, the truncation should also preserve the protecting symmetry in order for the classification to remain meaningful. This is consistent with recent works on the node structure in wavefunctions overlaps [19, 20], and we discuss their relation and distinction in the SM [21] Note that under certain truncation schemes, κ may no longer correspond to physical boundary phases for the truncated state. In such cases, truncation invariance remains true mathematically, but acquires a different physical interpretation, and may place the truncated state in a different topological class from the parent state, see later discussion on the parton construction of fractional Chern insulators.

Truncation invariance of Chern number and related topo-

logical indices—We begin by constructively showing that the Chern number is invariant under Hilbert space truncation. This serves as a generic proof that any topological index obtainable from a Chern number calculation will remain invariant under such a truncation. Calculation of the Chern number is at the heart of topological classification of two-parameter-family wavefunctions. In addition to the integer and fractional quantum Hall effect [10, 18, 22], it can also be used to classify symmetry protected topological (SPT) states by restricting its calculation to a subset of states or a reduced parameter space, examples include spin Chern number for time-reversal-invariant TIs [23–26], mirror Chern number [27] and more generally Chern numbers over 2D high symmetry manifold within a 3D single particle BZ for crystalline TIs [28]. We will discuss its implication on fractional Chern insulator states later in the text. A step by step illustration of the proof to be discussed below can be found in the SM [21] using a 3-band Hofstadter model. Further examples of band Chern insulators and Z_2 TIs are also provided in the SM [21].

Consider a gapped eigenstate of a many-body Hamiltonian in two dimensions, $|\Psi(\kappa)\rangle = \sum_{i=1}^M \Psi_i(\kappa)|B_i\rangle$, where $\kappa = (\kappa_x, \kappa_y)$ are twisted boundary phases, $\kappa_{x,y} \in [0, 2\pi)$. $\{|B_i\rangle\}$ are orthonormal many-body bases independent of κ , and $\Psi_i(\kappa) = \langle B_i|\Psi(\kappa)\rangle$ is periodic in κ . The Chern number of Ψ is $C = \frac{1}{2\pi} \iint_{\text{BZ}} d^2\kappa \nabla_\kappa \times \langle \Psi|i\nabla_\kappa|\Psi\rangle$. We first show that C can be computed using any two components of $|\Psi(\kappa)\rangle$, say $\Psi_{i_1}(\kappa)$ and $\Psi_{i_2}(\kappa)$, provided they do not vanish at the same κ point(s). We adopt the gauge fixing scheme of Ref. [22]. Assume for simplicity that a component $\Psi_{i_1}(\kappa)$ has a single zero in the entire BZ at, say, κ^* . Cases with multiple such zeros will be discussed later. Divide the BZ into two patches, where one patch, denoted as R_2 , is an infinitesimal neighborhood around κ^* , and the remainder of the BZ is the other patch, denoted as R_1 . We choose the gauge of $|\Psi\rangle$ such that

$$\Psi_{i_a}(\kappa) > 0 \text{ for } \kappa \in R_a, \quad a = 1, 2. \quad (1)$$

The gauge of $|\Psi\rangle$ is therefore smooth in both R_1 and R_2 , but has a phase mismatch across their interface,

$$|\Psi(\kappa_\cap)\rangle_{R_1} = e^{i\lambda(\kappa_\cap)} |\Psi(\kappa_\cap)\rangle_{R_2}, \quad \kappa_\cap \in R_1 \cap R_2, \quad (2)$$

where subscripts R_i denote gauge choice. In gauge R_1 , one can write $(\Psi_{i_1}, \Psi_{i_2})_{R_1} = (r_1, r_2 e^{i\chi})$ with $r_{1,2} > 0$ and real χ . Then under gauge R_2 , $(\Psi_{i_1}, \Psi_{i_2})_{R_2} = (r_1 e^{-i\chi}, r_2)$. By Eq. 2, one can identify $\lambda = \chi$, viz.,

$$\lambda(\kappa_\cap) = \text{Arg} [\Psi_{i_2}(\kappa_\cap)/\Psi_{i_1}(\kappa_\cap)], \quad (3)$$

which is *gauge invariant*. The BZ integral for computing C is now a sum over the two patches $R_{1,2}$, and by Stokes Theorem, each patch contributes a line integral of the Berry connection vector over the patch's boundary, thus

$$C = \frac{1}{2\pi} \sum_{i=1,2} \oint_{\partial R_i} d\kappa_\cap \cdot \langle \Psi|i\nabla_{\kappa_\cap}|\Psi\rangle_{R_i} = w[\lambda], \quad (4)$$

where $w[\lambda] = \frac{1}{2\pi} \oint_{\partial R_2} d\kappa_\cap \cdot \partial_{\kappa_\cap} \lambda$ is the winding number of the phase mismatch $\lambda(\kappa_\cap)$ in the counter-clockwise direction—note that the two boundaries, ∂R_1 and ∂R_2 , are identical but in opposite directions. If Ψ_{i_1} has multiple zeros, one can define a phase mismatch λ_a around the a^{th} zero, and $C = \sum_a w[\lambda_a]$. Eqs. 3 and 4 together establish that the Chern number of $|\Psi\rangle$ can be computed using any two of its components.

Now consider a truncated state $|\tilde{\Psi}\rangle$ obtained by taking a subset of wavefunction components from $|\Psi\rangle$ and renormalizing. Its Chern number can be computed in the same way using $\tilde{\Psi}_{i_1}$ and $\tilde{\Psi}_{i_2}$. Since both are simply rescaled from their pre-truncation values, the phase mismatch (Eq. 3) is not affected by the truncation, hence $|\tilde{\Psi}\rangle$ and $|\Psi\rangle$ have the same Chern number.

Truncation invariance of quantized Berry phase—Symmetry-protected 1D topological phases exhibit a robust Z_2 index due to the quantization of the Berry phase to either 0 or π . We now prove the truncation invariance of the Z_2 class protected by inversion-like symmetries. Examples in this class include the Su-Schrieffer-Heeger model, Kitaev's p -wave superconductor, and Spin-1 antiferromagnetic chain. Consider a parent many-body Hamiltonian $H(\kappa) = H(\kappa + 2\pi)$, where $\kappa \in [0, 2\pi)$ is the boundary phase. Inversion-like invariance is defined as $SH(\kappa)S^{-1} = H(-\kappa)$ where the unitary S represents the symmetry operation. At the symmetry invariant points $\kappa_{\text{SIP}} \in \{0, \pi\}$, S commutes with $H(\kappa_{\text{SIP}})$, hence the ground state of H , assumed unique, must also be a symmetry eigenstate, $S|\Psi(\kappa_{\text{SIP}})\rangle = s_{\kappa_{\text{SIP}}}|\Psi(\kappa_{\text{SIP}})\rangle$, where $s_{\kappa_{\text{SIP}}} = \pm 1$. Hughes *et al* showed [29] that the Berry phase of $|\Psi(\kappa)\rangle$ can be computed from the symmetry eigenvalues at κ_{SIP} , $e^{i\gamma} = s_0 s_\pi$. Now consider a truncation P that preserves inversion, $[P, S] = 0$. It follows that the truncated state $P|\Psi(\kappa_{\text{SIP}})\rangle$ remains an inversion eigenstate with the same eigenvalue $s_{\kappa_{\text{SIP}}}$ as the parent state $|\Psi(\kappa_{\text{SIP}})\rangle$. Hence, the Berry phase also remains invariant, provided P does not annihilate $|\Psi(\kappa)\rangle$ for any κ .

Parton construction of fractional Chern insulators—Truncation invariance of the Chern number is closely related to the parton construction of fractional Chern insulator (FCI) states [30–34]. Consider the $\text{SU}(m)$ FCI state [30, 31], a lattice analogue of the Laughlin $\frac{1}{m}$ state. One writes the electron (or boson) operator as a product of m partons, $c_r = \prod_{\alpha=1}^m f_r^{(\alpha)}$. Each parton species is subjected to a tight binding Hamiltonian with lowest band Chern number 1. Filling one band per species then leads to a parton mean field state $|\Psi_{\text{MF}}\rangle$ with Chern number $C_{\text{MF}} = m$ by construction. The FCI state is obtained by Gutzwiller projecting $|\Psi_{\text{MF}}\rangle$ back to the electron Hilbert space, $|\Psi_{\text{el}}\rangle \propto P_G|\Psi_{\text{MF}}\rangle$, that is, 0 or m partons per lattice site. From truncation invariance, $|\Psi_{\text{el}}\rangle$ and $|\Psi_{\text{MF}}\rangle$ have the same Chern number over a parton BZ, $\kappa_{x,y} \in [0, 2\pi)$. Here, $\kappa_{x,y}$ are parton twisted boundary phases, $f_{r+N_i\hat{e}_i}^{(\alpha)} = e^{i\kappa_i} f_r^{(\alpha)}$. The corresponding boundary conditions for electrons are $c_{r+N_i\hat{e}_i} = \prod_{\alpha=1}^m f_{r+N_i\hat{e}_i}^{(\alpha)} = e^{im\kappa_i} c_r$, hence one parton BZ is equivalent to m^2 electron BZs. Thus although the Chern number remains invariant after truncation when computed using the parton BZ,

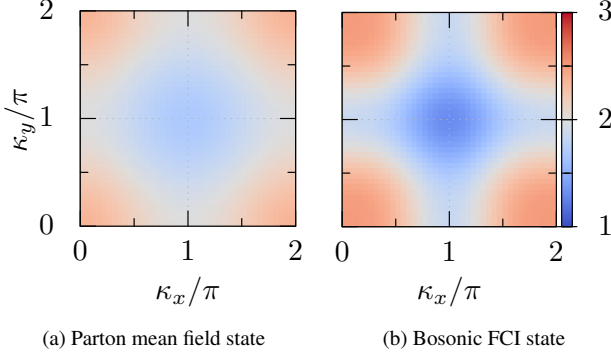


FIG. 1. Chern number density in the space of parton boundary phases for (a) the parent (untruncated) parton mean-field state, and (b) the bosonic fractional Chern insulator state obtained via Gutzwiller projection. In both cases, the Chern number density integrates to the same $C_{MF} = 2$ over the parton BZ, as required by truncation invariance. The physical Hall conductance of the FCI state is given by $C = \frac{C_{MF}}{m^2} = \frac{1}{2}$ with $m = 2$ parton species, see text for detail. Calculation is done with a 4×4 lattice and a 40×40 grid of (κ_x, κ_y) .

the physical Hall conductance is related to the Chern number per electron BZ [18], and we recover the fractional Hall conductance of $|\Psi_{el}\rangle$ as $C = \frac{C_{MF}}{m^2} = \frac{1}{m}$.

In Fig. 1, we use the π -flux square lattice model of Ref. [32] as the mean field Hamiltonian for $m = 2$ parton species, and plot the Chern number density for both the untruncated parton mean field state $|\Psi_{MF}\rangle$ and the bosonic FCI state obtained by Gutzwiller projecting $|\Psi_{MF}\rangle$ to 0 or 2 partons per site. In both cases, the Chern number density integrates to $C_{MF} = 2$ over the parton BZ, as guaranteed by truncation invariance. The physical Hall conductance is given by $C = \frac{C_{MF}}{m^2} = \frac{1}{2}$.

We note that numerical calculations of the fractional Chern number of Gutzwiller-projected parton states are severely limited by system size [33]. Our theorem establishes such results on a more general ground, without system size restriction. The same argument applies to the ground states of non-Abelian FCIs as well (see SM [21]), although its connection with quasi-particle statistics remains an open question.

Spin-1 antiferromagnetic chain—We use the Spin-1 AKLT and Heisenberg models to illustrate truncation invariance of the quantized Berry phase [35, 36]. The Hamiltonian is $H(\kappa) = \sum_{i=1}^N \mathbf{S}_i \cdot \mathbf{S}_{i+1} + \beta(\mathbf{S}_i \cdot \mathbf{S}_{i+1})^2$, where κ is a boundary phase: $S_{N+1}^\pm = S_1^\pm e^{\mp i\kappa}$ and $S_{N+1}^z = S_1^z$. Define inversion \mathcal{I} as $\mathcal{I}S_i\mathcal{I}^{-1} \equiv S_{N+1-i}$, then $H(\kappa)$ is inversion symmetric, $\mathcal{I}H(\kappa)\mathcal{I}^{-1} = H(-\kappa)$. For $|\beta| < 1$, its gapped ground state $|\Psi(\kappa)\rangle$ has a nontrivial Z_2 index characterized by a quantized π Berry phase. We first consider the AKLT $\beta = \frac{1}{3}$, for which $|\Psi(\kappa)\rangle$ can be obtained analytically [37, 38], $|\Psi(\kappa)\rangle = \prod_{i=1}^N (a_i^\dagger b_{i+1}^\dagger - b_i^\dagger a_{i+1}^\dagger) |\emptyset\rangle$, where a and b are Schwinger bosons, $S_i^+ = a_i^\dagger b_i$, $S_i^z = \frac{1}{2}(a_i^\dagger a_i - b_i^\dagger b_i)$, $a_i^\dagger a_i + b_i^\dagger b_i \stackrel{!}{=} 2$, $|\emptyset\rangle$ is the boson vacuum, and $(a_{N+1}, b_{N+1}) = (a_1, b_1 e^{-i\kappa})$. Now project $|\Psi(\kappa)\rangle$ onto two inversion conjugate spin configurations $|B\rangle = |s_1^z, s_2^z, \dots, s_N^z\rangle$ and $|\bar{B}\rangle = \mathcal{I}|B\rangle$, $s_i^z \in \{0, \pm 1\}$. To have $\langle B|\Psi(\kappa)\rangle \neq 0$, the nonzero spins in $|B\rangle$ must have

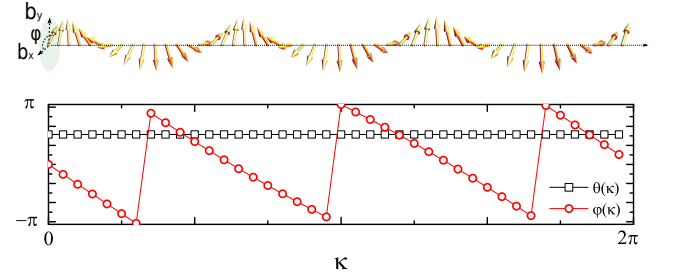


FIG. 2. Projected Heisenberg ground state. (Top) Schematic plot showing the helical precession of the Bloch vector parametrizing the projected state, $|\tilde{\Psi}\rangle = \cos \frac{\theta}{2} |B\rangle + \sin \frac{\theta}{2} e^{i\varphi} |\bar{B}\rangle$. (Bottom) Spherical angles φ and θ . Over the cycle $\kappa = 0 \rightarrow 2\pi$, θ remains a constant $\frac{\pi}{2}$, and $\varphi(\kappa)$ changes by -6π , hence the winding number of \bar{b} is -3 , consistent with a Berry phase of $\pi(\text{mod } 2\pi)$. $N = 12$ spin-1 sites are used. The ground state is truncated to the many-body basis $|B\rangle = |\uparrow\uparrow\uparrow\uparrow 0 \downarrow\downarrow\downarrow\downarrow 0\rangle$ and its inversion partner.

alternating signs, a manifestation of string order [39, 40]. One can show that the normalized truncated wavefunction is $|\tilde{\Psi}(\kappa)\rangle = \frac{1}{\sqrt{2}}(|B\rangle + (-1)^N e^{i s \kappa} |\bar{B}\rangle)$, where s is the leftmost nonzero spin in configuration $|B\rangle$. This form is largely fixed by the inversion conjugacy between $|B\rangle$ and $|\bar{B}\rangle$, which ensures that (1) they have the same number of nonzero spins, and hence are of equal absolute weight, and (2) their leftmost nonzero spins are opposite, which leads to the relative phase $e^{i s \kappa}$. Spoiling either condition will lead to a non-quantized Berry phase. See SM [21] for derivation. Parametrized on a Bloch sphere, $|\tilde{\Psi}\rangle$ lies on the equator and manifestly has a winding number $w_{\tilde{\Psi}} = s$, hence its Berry phase is $s\pi \equiv \pi \text{ mod } 2\pi$.

When $\beta \neq \frac{1}{3}$, the Hamiltonian is no longer a projection operator onto bond singlets, hence there is a proliferation of spin configurations in the ground state that violate the sign-alternating string order, and the winding number of a truncated state, $w_{\tilde{\Psi}}$, is not restricted to ± 1 . Nevertheless, since inversion symmetry is intact, the post-truncation Berry phase remains π , indicating that $w_{\tilde{\Psi}}$ is an odd integer. Using the Heisenberg model ($\beta = 0$), we have numerically verified that (1) if $|B\rangle$ and $|\bar{B}\rangle$ are string ordered, the winding number remains ± 1 ; if not, the winding number is an odd integer but not necessarily ± 1 , see Fig. 2. (2) If we instead twist the Hamiltonian on the bond between S_ℓ and $S_{\ell+1}$, the new winding number $w_{\tilde{\Psi}}^{(\ell)}$ is related to $w_{\tilde{\Psi}}$ via a ‘‘Gauss law’’, $w_{\tilde{\Psi}}^{(\ell)} - w_{\tilde{\Psi}} = -2 \sum_{n=1}^{\ell} s_n^z$, suggesting that $s_n^z = \pm 1$ in a given spin configuration act as charge ∓ 2 sources of winding numbers. (3) For projections that violate inversion symmetry, the Berry phase is in general not quantized any more. These results are numerically robust even though the typical weight on a many-body basis state is exponentially small ($\sim \frac{1}{\sqrt{3^N}}$).

Relation with bulk entanglement—Connection between Hilbert space truncation and topology has previously been studied from the perspective of quantum entanglement [29, 41–47]. We briefly discuss the relation between entanglement and wavefunction truncation in the context of bulk entangle-

ment [48–52] due to a sublattice bipartition. Consider a single occupied Bloch band $|\psi_k\rangle$ with momentum \mathbf{k} . Generalization to multiple occupied bands is straightforward. The Schmidt decomposition of $|\psi_k\rangle$ into two sublattice groups A and B is

$$|\psi_k\rangle = \sqrt{f_k}|\tilde{\psi}_{A,k}\rangle \otimes |\emptyset_B\rangle + \sqrt{1-f_k}|\emptyset_A\rangle \otimes |\tilde{\psi}_{B,k}\rangle, \quad (5)$$

where $|\emptyset_{A(B)}\rangle$ and $|\tilde{\psi}_{k,A(B)}\rangle$ are respectively the vacuum and the truncated state in part $A(B)$, $f_k = \langle\psi_k|P_A|\psi_k\rangle$. $|\tilde{\psi}_{k,A}\rangle$ is thus an entanglement eigenstate for part A in the single particle sector, with entanglement eigenvalue f_k . For a partition with N_A sublattices in A , there should be a total of N_A (single particle) entanglement levels, thus $N_A - 1$ of them are identically zero. If $f_k \neq 0 \forall \mathbf{k}$, it is gapped from the remainder, hence one can introduce a topological index, such as an entanglement Chern number [49], for the corresponding entanglement eigenstate, *i.e.*, the truncated state $|\tilde{\psi}_{k,A}\rangle$. Truncation invariance thus implies that the *entanglement topological index* must be identical to the topological index of the parent state if (1) the bulk entanglement spectrum is gapped from zero, and (2) for SPT parent states, the entanglement partition preserves the protecting symmetry.

Measuring topological index via partial tomography—Truncation invariance of the topological index is experimentally relevant. Recent breakthrough in quench-based quantum tomography has made it possible to extract topological indices of *two*-component Bloch wavefunctions by performing a full measurement of both wavefunction components over the entire BZ (of Bloch momenta) [53, 54]. We now discuss a quench-based partial quantum tomography for a multi-component Bloch wavefunction $|\psi(\mathbf{k})\rangle = \sum_{a=1}^N \psi_a(\mathbf{k})|a\rangle$, from which two chosen components $\psi_{a_1}(\mathbf{k})$ and $\psi_{a_2}(\mathbf{k})$ can be measured. Here a labels sublattices within a unit cell. Combined with truncation invariance, this allows us to determine the Chern number of the full state $|\psi(\mathbf{k})\rangle$. We follow the experimental protocol of Refs. [53, 54]. Assume at $t = 0$ the system has been prepared as a filled Bloch band described by $|\psi(\mathbf{k})\rangle$. For $0 < t < t_h$, we quench the system with a flat band Hamiltonian $H(\mathbf{k}) = \sum_{a=1}^N \varepsilon_a |a\rangle\langle a|$. The values of $\{\varepsilon_a\}$ will be specified later. At the end of the quench, one has $|\psi(\mathbf{k}, t_h)\rangle = \sum_{a=1}^N \psi_a(\mathbf{k}, t_h)|a\rangle$ where $\psi_a(\mathbf{k}, t_h) = \psi_a(\mathbf{k})e^{-i\varepsilon_a t_h}$. The system is then released for a time of flight (TOF) measurement. The resulting momentum distribution from the TOF analysis is given by [53] $n(\mathbf{k}, t_h) = \left|\sum_{a=1}^N \psi_a(\mathbf{k}, t_h)\right|^2$, and by monitoring $n(\mathbf{k}, t_h)$ as a continuous function of t_h , contributions from different $\psi_a(\mathbf{k})$ (at $t = 0$) can in principle be resolved.

To perform a partial tomography on, say, the first two sublattices $a = 1, 2$, we set ε_a for all other sublattices $a > 2$ to a common level E , and require that $\varepsilon_1 \neq \varepsilon_2 \neq E$. Consequently, the momentum distribution $n(\mathbf{k}, t_h)$ has only three distinctive frequency modes,

$$\omega_{1(2)} = \varepsilon_{1(2)} - E, \quad \omega_3 = \varepsilon_2 - \varepsilon_1, \quad (6)$$

and from the TOF experiment, one can extract the correspond-

ing Fourier coefficients A_i, B_i ,

$$n(\mathbf{k}, t_h) = A_0(\mathbf{k}) + \sum_{i=1}^3 \left[A_i(\mathbf{k}) \cos(\omega_i t_h) + B_i(\mathbf{k}) \sin(\omega_i t_h) \right]. \quad (7)$$

Parametrize $\psi_1 = u \sin \frac{\theta}{2}$ and $\psi_2 = -u \cos \frac{\theta}{2} e^{i\varphi}$, $u > 0$. The overall scale u does not enter the topological index evaluation. The Bloch vector angles φ and θ are

$$\tan \varphi(\mathbf{k}) = \frac{B_3(\mathbf{k})}{A_3(\mathbf{k})}, \quad \tan \frac{\theta(\mathbf{k})}{2} = \sqrt{\frac{A_1^2(\mathbf{k}) + B_1^2(\mathbf{k})}{A_2^2(\mathbf{k}) + B_2^2(\mathbf{k})}}, \quad (8)$$

see SM [21] for derivation and φ, θ plots of a truncated Hofstadter band. Eq. 8 allows us to extract the projected state $|\tilde{\psi}\rangle = (\frac{\psi_1}{u}, \frac{\psi_2}{u})'$, from which the Chern number of the full state can be computed. In fact, since $|\tilde{\psi}\rangle$ is also a bulk entanglement eigenstate, this is a measurement protocol for the entanglement Chern number of a sublattice truncation as discussed in the previous section.

Conclusion—We have shown that a normalizable truncated wavefunction preserves the topological index of its parent state, if both indices are computed in the space of the parent state’s twisted boundary phases. The physical interpretation of the index may change for the truncated state if its boundary condition is affected by the truncation, and we gave an example using the parton construction of the $SU(m)$ FCI state. We also showed that a sublattice-truncated state can be identified as an entanglement eigenstate resulting from a sublattice bipartition, revealing a connection between wavefunction truncation and quantum entanglement. Our finding provides a new perspective on the topological structure of wavefunctions, and indicates that mathematical specification of a topological index, and perhaps even its physical manifestation, can be achieved in a much smaller Hilbert space, such as the 2-sublattice space that may be probed by the partial tomography scheme discussed in the text.

Acknowledgments—We are grateful to Yi Zhang for critical reading and comments of an early draft, and to D. N. Sheng, Kai Sun, Christof Weitenberg, Avadh Saxena, Hongchul Choi, and S. Kourtis for useful discussions and communications. W.Z. thanks T. S. Zeng for helpful discussion and F. D. M. Haldane for education of the physics of spin-1 antiferromagnetic chain. Work at LANL was supported in part by US DOE BES E3B7 (ZSH, JXZ, and AVB), US DOE NNSA through LANL LDRD (ZSH, WZ, and AVB), and the CINT, a US DOE BES user facility (JXZ). Work at NORDITA was supported by ERC DM 321031 (AVB).

* zsh@lanl.gov

† zhuwei@lanl.gov

‡ darovas@ucsd.edu

§ jxzh@lanl.gov

¶ avb@nordita.org

- [1] B. A. Bernevig and T. L. Hughes, *Topological Insulators and Topological Superconductors* (Princeton University Press, 2013).
- [2] X.-L. Qi and S.-C. Zhang, *Rev. Mod. Phys.* **83**, 1057 (2011).
- [3] S. Ryu, A. P. Schnyder, A. Furusaki, and A. W. W. Ludwig, *New Journal of Physics* **12**, 065010 (2010), arXiv:0912.2157 [cond-mat.mes-hall].
- [4] C.-K. Chiu, J. C. Y. Teo, A. P. Schnyder, and S. Ryu, *Rev. Mod. Phys.* **88**, 035005 (2016).
- [5] M. Z. Hasan and C. L. Kane, *Rev. Mod. Phys.* **82**, 3045 (2010).
- [6] Y. Ando, *Journal of the Physical Society of Japan* **82**, 102001 (2013), arXiv:1304.5693 [cond-mat.mtrl-sci].
- [7] I. Bloch, J. Dalibard, and W. Zwerger, *Rev. Mod. Phys.* **80**, 885 (2008).
- [8] I. Bloch, J. Dalibard, and S. Nascimbène, *Nature Physics* **8**, 267 (2012).
- [9] T. Langen, R. Geiger, and J. Schmiedmayer, *Annual Review of Condensed Matter Physics* **6**, 201 (2015), arXiv:1408.6377 [cond-mat.quant-gas].
- [10] D. J. Thouless, M. Kohmoto, M. P. Nightingale, and M. den Nijs, *Phys. Rev. Lett.* **49**, 405 (1982).
- [11] J. Zak, *Phys. Rev. Lett.* **62**, 2747 (1989).
- [12] R. D. King-Smith and D. Vanderbilt, *Phys. Rev. B* **47**, 1651 (1993).
- [13] K. Suzuki and S. Y. Lee, *Progress of Theoretical Physics* **64**, 2091 (1980).
- [14] P. W. Anderson, *Science* **235**, 1196 (1987).
- [15] C. Gros, *Annals of Physics* **189**, 53 (1989).
- [16] U. Schollwöck, *Annals of Physics* **326**, 96 (2011), arXiv:1008.3477 [cond-mat.str-el].
- [17] X.-G. Wen, *Phys. Rev. B* **65**, 165113 (2002).
- [18] Q. Niu, D. J. Thouless, and Y.-S. Wu, *Phys. Rev. B* **31**, 3372 (1985).
- [19] J. Gu and K. Sun, *Phys. Rev. B* **94**, 125111 (2016), arXiv:1605.07627 [cond-mat.str-el].
- [20] Z. Huang and A. V. Balatsky, *Phys. Rev. Lett.* **117**, 086802 (2016), arXiv:1604.04698 [cond-mat.stat-mech].
- [21] See Supplemental Materials [url] for additional examples and derivation details, which includes additional Refs. [55–59].
- [22] M. Kohmoto, *Annals of Physics* **160**, 343 (1985).
- [23] D. N. Sheng, Z. Y. Weng, L. Sheng, and F. D. M. Haldane, *Phys. Rev. Lett.* **97**, 036808 (2006).
- [24] T. Fukui and Y. Hatsugai, *Phys. Rev. B* **75**, 121403 (2007).
- [25] E. Prodan, *Phys. Rev. B* **80**, 125327 (2009).
- [26] Y. Yang, Z. Xu, L. Sheng, B. Wang, D. Y. Xing, and D. N. Sheng, *Phys. Rev. Lett.* **107**, 066602 (2011).
- [27] J. C. Y. Teo, L. Fu, and C. L. Kane, *Phys. Rev. B* **78**, 045426 (2008).
- [28] A. Alexandradinata, C. Fang, M. J. Gilbert, and B. A. Bernevig, *Phys. Rev. Lett.* **113**, 116403 (2014).
- [29] T. L. Hughes, E. Prodan, and B. A. Bernevig, *Phys. Rev. B* **83**, 245132 (2011).
- [30] J. McGreevy, B. Swingle, and K.-A. Tran, *Phys. Rev. B* **85**, 125105 (2012).
- [31] Y.-M. Lu and Y. Ran, *Phys. Rev. B* **85**, 165134 (2012).
- [32] Y. Zhang and A. Vishwanath, *Phys. Rev. B* **87**, 161113 (2013).
- [33] W.-J. Hu, W. Zhu, Y. Zhang, S. Gong, F. Becca, and D. N. Sheng, *Phys. Rev. B* **91**, 041124 (2015).
- [34] S. Kourtis, T. Neupert, C. Chamon, and C. Mudry, *Phys. Rev. Lett.* **112**, 126806 (2014).
- [35] F. D. M. Haldane, *Phys. Rev. Lett.* **50**, 1153 (1983).
- [36] T. Hirano, H. Katsura, and Y. Hatsugai, *Phys. Rev. B* **77**, 094431 (2008).
- [37] I. Affleck, T. Kennedy, E. H. Lieb, and H. Tasaki, *Phys. Rev. Lett.* **59**, 799 (1987).
- [38] D. P. Arovas, R. N. Bhatt, F. D. M. Haldane, P. B. Littlewood, and R. Rammal, *Phys. Rev. Lett.* **60**, 619 (1988).
- [39] K. Rommelse and M. den Nijs, *Phys. Rev. Lett.* **59**, 2578 (1987).
- [40] S. M. Girvin and D. P. Arovas, *Physica Scripta* **1989**, 156 (1989).
- [41] I. Peschel, *Journal of Physics A: Mathematical and General* **36**, L205 (2003).
- [42] S.-A. Cheong and C. L. Henley, *Phys. Rev. B* **69**, 075111 (2004).
- [43] H. Li and F. D. M. Haldane, *Phys. Rev. Lett.* **101**, 010504 (2008).
- [44] R. Thomale, D. P. Arovas, and B. A. Bernevig, *Phys. Rev. Lett.* **105**, 116805 (2010).
- [45] F. Pollmann, A. M. Turner, E. Berg, and M. Oshikawa, *Phys. Rev. B* **81**, 064439 (2010).
- [46] E. Prodan, T. L. Hughes, and B. A. Bernevig, *Physical Review Letters* **105**, 115501 (2010), arXiv:1005.5148 [cond-mat.mes-hall].
- [47] Z. Huang and D. P. Arovas, *Phys. Rev. B* **86**, 245109 (2012), arXiv:1201.0733 [cond-mat.stat-mech].
- [48] T. H. Hsieh and L. Fu, *Phys. Rev. Lett.* **113**, 106801 (2014).
- [49] T. Fukui and Y. Hatsugai, *Journal of the Physical Society of Japan* **83**, 113705 (2014).
- [50] D.-W. Chiou, H.-C. Kao, and F.-L. Lin, *Phys. Rev. B* **94**, 235129 (2016).
- [51] M. Legner and T. Neupert, *Phys. Rev. B* **88**, 115114 (2013).
- [52] J. Schliemann, *New Journal of Physics* **15**, 053017 (2013), arXiv:1302.5517 [cond-mat.stat-mech].
- [53] P. Hauke, M. Lewenstein, and A. Eckardt, *Physical Review Letters* **113**, 045303 (2014), arXiv:1401.8240 [cond-mat.quant-gas].
- [54] N. Fläschner, B. S. Rem, M. Tarnowski, D. Vogel, D.-S. Lühmann, K. Sengstock, and C. Weitenberg, *Science* **352**, 1091 (2016), arXiv:1509.05763 [cond-mat.quant-gas].
- [55] D. R. Hofstadter, *Phys. Rev. B* **14**, 2239 (1976).
- [56] B. A. Bernevig, T. L. Hughes, and S.-C. Zhang, *Science* **314**, 1757 (2006).
- [57] R. Yu, X. L. Qi, A. Bernevig, Z. Fang, and X. Dai, *Phys. Rev. B* **84**, 075119 (2011).
- [58] C. Weitenberg, Private communication.
- [59] Y.-F. Wang, H. Yao, Z.-C. Gu, C.-D. Gong, and D. N. Sheng, *Phys. Rev. Lett.* **108**, 126805 (2012).